RSC Advances

PAPER

Cite this: *RSC Adv.*, 2021, **11**, 14932

Synthesis and characterization of biobased thermoplastic polyester elastomers containing Poly(butylene 2,5-furandicarboxylate)†

Hailan Kang, *[ab] Xiaoli Miao,[ab] Jiahuan Li,[ab] Donghan Li[ab] and Qinghong Fang*[ab]

A series of sustainable and reprocessible thermoplastic polyester elastomers P(BF-PBSS)s were synthesized using dimethyl-2,5-furandicarboxylate, 1,4-butanediol, and synthetic low-molecular-weight biobased polyester (PBSS). The P(BF-PBSS)s contain poly(butylene 2,5-furandicarboxylate) (PBF) as their hard segment and PBSS as their soft segment. The microstructures of the P(BF-PBSS)s were confirmed by nuclear magnetic resonance, demonstrating that a higher content of the soft segment was incorporated into P(BF-PBSS)s with higher PBSS content. Interestingly, dynamic mechanical analysis indicated that P(BF-PBSS)s comprised two domains: crystalline PBF and a mixture of amorphous PBF and PBSS. Consequently, the microphase separations of P(BF-PBSS)s were mainly induced by the crystallization of their PBF segments. More importantly, the thermal, crystallization, and mechanical properties could be tailored by tuning the PBSS content. Our results indicate that the as-prepared P(BF-PBSS)s are renewable, thermally stable, and nontoxic, and have good tensile properties, indicating that they could be potentially applied in biomedical materials.

Received 4th January 2021
Accepted 15th April 2021

DOI: 10.1039/d1ra00066g

rsc.li/rsc-advances

1. Introduction

Recently, interest in the development of ecofriendly polymeric materials has been rapidly growing owing to increasing environmental awareness, the depletion of fossil fuel reserves, and the price fluctuations of these materials.[1–4] Biobased polymers, especially aliphatic polyesters, such as polylactic acid (PLA), poly(3-hydroxyalkanoate)s, and poly(butylene succinate), have already been successfully commercialized, providing sustainable alternatives to traditional petroleum-based polymers.[5–7]

Thermoplastic polyester elastomers (TPEEs) are a class of polymers that combine the high processability of thermoplastics with the elasticity of elastomers.[8–13] Generally, TPEEs contain a hard crystalline segment and a soft amorphous segment. The crystalline segments, which typically consist of multiple short-chain esters (such as butylene terephthalate units), provide TPEEs with a high melting temperature, excellent crystallization, and good mechanical properties. At the same time, the amorphous segments, which are derived from polyether and polyester glycols, provide high flexibility and elasticity. Further, the crystallization of the crystalline segments of TPEEs induces microphase separation of the hard and soft segments. The microphase separation results in the rigid hard segment acting as a physical cross-link, whereas flexible soft segment acts as a reversible network. As a result, the thermal and mechanical properties of TPEEs can be finely regulated *via* the hard and soft segment types and compositions. The first commercial TPEE was marketed as Hytrel® by DuPont in 1972, and it contained polybutylene terephthalate (PBT) as its hard segment.[14] Owing to their excellent performance, TPEEs have since been applied in a variety of automotive and electronic applications as well as in biomedicine. These commercial TPEEs, however, are dependent on petroleum-based chemicals, and therefore the green and sustainable development of TPEEs is an urgent necessity.

Significant efforts have been made in this respect using renewable monomers as a means of synthesizing aliphatic thermoplastic elastomers.[15–25] Recently, polylactide-based copolymers, such as PLA-*b*-polymyrcene-*b*-PLA,[15] PLA-*b*-poly(6-methyl-ε-caprolactone)-*b*-PLA,[16] and PLA-poly(dimer acid methyl ester-*alt*-poly(propylene glycol))-PLA,[17] PLA-*b*-poly(ε-caprolactone-*co*-ε-decalactone)-*b*-PLA,[18] PLA-polymenthide-PLA,[19] among others, have been successfully developed as sustainable alternatives to petroleum-based TPEE. Some biobased TPEEs have been demonstrated unsatisfactory performance, such as low modulus and strength. Therefore, there is a strong need to introduce sustainable monomers for the development of additional types of biobased TPEEs.

[a]*College of Materials Science and Engineering, Shenyang University of Chemical Technology, Shenyang, 110142, China. E-mail: kanghailan@syuct.edu.cn; fqh80@126.com*

[b]*Key Laboratory for Rubber Elastomer of Liaoning Province, Shenyang University of Chemical Technology, Shenyang, 110142, China*

† Electronic supplementary information (ESI) available: Fig. S1. The GPC curve of PBF and P(BF-PBSS)s; Fig. S2. RGR values of PBF and P(BF-PBSS)s at different incubation time; Table S1. Thermal properties of PBF and P(BF-PBSS)s; Table S2. Relationship between cell relative growth rate (RGR) and cytotoxicity grade of a material. See DOI: 10.1039/d1ra00066g

Rigid biobased chemicals, such as isosorbide[26] and 2,5-furandicarboxylic acid,[27] have been introduced into the polymeric chains of aliphatic polyesters to improve their properties. However, the poor reactivity of the secondary hydroxyl group of isosorbide resulted in low number-average molecular weights in the produced copolyesters.[28–30] 2,5-Furandicarboxylic acid (FDCA) is another highly promising biobased chemical. It has a furan ring and can be derived from polysaccharide or sugar. In particular, FDCA stands out as an ideal biobased substitute to terephthalic acid because of its rigid aromatic ring structure. Because it is biobased and may have superior performance, FDCA has previously been adapted to synthesize biobased homopolyesters and copolyesters.[30–42] For example, Chi *et al.* prepared a novel biobased TPEE by polymerizing dimethyl 2,5-furandicarboxylate, neopentyl, and poly(tetramethylene glycol), identifying that poly(neopentyl glycol 2,5-furandicarboxylate) as a promising hard segment owing to its high melting temperature and good crystallizability.[35] Xie *et al.* developed poly(-ethylene 2,5-furandicarboxylate-*mb*-poly(tetramethylene glycol)) copolymers (P(EF-*mb*-PTMG)), and the performance could be tailored by tuning the PTMG content.[37] In addition, Sousa *et al.* synthesized poly(1,4-butylene 2,5-furandicarboxylate) (PBF)/poly(ethylene glycol) copolyesters that demonstrated improved processing features compared with PBF.[36] Further, Zheng *et al.* produced multi-blocked biobased copolyesters using PBF as the hard segment and ε-caprolactone polyester diol as soft segment.[38]

Although biobased polyester elastomers from biobased diols and diacids have been recently reported,[43–46] they are thermosetting, meaning they cannot be reprocessed once molded. Interestingly, research findings regarding these elastomers indicate that miscellaneous biobased reacting monomers would result in amorphous elastomers. Given this context, we developed herein an amorphous low-molecular-weight hydroxyl-terminated copolyester (PBSS) by polymerizing biobased monomers containing 1,3-propanediol, 1,4-butanediol, sebacic acid and succinic acid. A series of biobased TPEEs, called P(BF-PBSS)s, were then designed and synthesized using PBF as the hard segment and PBSS as the soft segment. The chemical structure, thermal and mechanical properties, and cytocompatibilty of the P(BF-PBSS)s were systematically investigated. Further, the properties of the P(BF-PBSS)s were modulated by tuning the hard and soft segment compositions.

2. Experimental section

2.1. Materials

1,3-Propanediol (PDO, 99%), 1,4-butanediol (BDO, 99%), sebacic acid (SeA, 99%), succinic acid (SuA, 99%), tetrabutyl titanate (TBT, 99%), phenol (AR), and *p*-hydroxyanisole (99%) were purchased from Tianjin Damao Chemical Reagent Factory (China). Dimethyl-2,5-furandicarboxylate (DMFD, ≥98%) was purchased from Wuhan Yuancheng Gongchuang Technology Co. Ltd, China. PDO and SeA are produced by starch and castor oil, respectively. According to the supplier, SeA was produced *via* castor oil by cracking method, and DMFD was produced *via* oxidation of 5-hydroxymethylfurfural which is derived from the dehydration of C6 sugars. PDO, BDO, and SuA can been industrially produced by fermentation of starch or glucose. Chloroform, methanol, tetrachloroethane and *N*,*N*-dimethyl formamide (DMF) were purchased from Tianjin Yongda Chemical Reagent Co. Ltd, China. All chemicals were used as received without further purification.

2.2. Synthesis of low-molecular-weight polyester

Low-molecular-weight hydroxyl-terminated copolyester (PBSS) was synthesized according to the methods described in previous studies.[43] The synthetic process can be briefly described as follows. First, PDO (27.39 g, 0.36 mol), BDO (32.44 g, 0.36 mol), SuA (49.60 g, 0.42 mol), SeA (36.41 g, 0.18 mol), and the antioxidant *p*-hydroxyanisole (0.2917 g) were added to the reactor and reacted for 2 h at 180 °C under a N_2 atmosphere. Then, the catalyst (TBT, 0.05 wt% relative to the total monomer weight) was added, and the reaction was carried out for 1 h at 180 °C under reduced pressure conditions. Finally, the extra BDO was added to the system to obtain the hydroxyl-terminated PBSS. The obtained product was dissolved in chloroform, precipitated in excess cold methanol, and dried under vacuum conditions. PBSS exhibited a number-average molecular weight of 3044, a polydispersity index of 1.23, and a glass transition temperature of −55 °C. The molar ratio of PDO/BDO/SuA/SeA were 0.28 : 0.32 : 0.28 : 0.12, which was calculated by ^{1}H-NMR of PBSS.

2.3. Synthesis of P(BF-PBSS)s

Copolyesters have generally been synthesized using transesterification and melt polycondensation reactions,[35,38] and we used the same method in this study. Briefly, DMFD (18.44 g, 100.0 mmol), BDO (11.48 g, 127.4 mmol), PBSS (7.90 g, 2.60 mmol), and *p*-hydroxyanisole (0.076 g) were reacted together at 160 °C for 1 h under a N_2 atmosphere. The mixtures were then heated to 170 °C for 1 h and continually heated to 180 °C for 2 h. Next, TBT (0.1 wt% relative to the total monomer weight) was added, the temperature was raised to 220 °C under reduced pressure conditions, and the mixtures were reacted for 4–6 h. The prepared copolyesters are referred to as P(BF-PBSS)-*m*, and *m* indicates the weight fraction of PBSS, which is calculated according to eqn (1).

$$m = \frac{m_{\mathrm{PBSS}}}{m_{\mathrm{PBSS}} + m_{\mathrm{DMFD}}} \quad (1)$$

where m_{PBSS} and m_{DMFD} are the mass of PBSS and DMFD in feed, respectively.

2.4. Characterization

The molecular weights of P(BF-PBSS)s were measured by gel permeation chromatography (GPC; Agilent PL-GPC 50, Agilent Technologies Inc., USA) using DMF as the eluent at 100 °C. The molecular weight of PBSS was tested by GPC (Waters 2410 RI Detector, Waters Co., USA) using tetrahydrofuran as the eluent at 40 °C.

Nuclear magnetic resonance (NMR) spectra were recorded on a Bruker AVANCE III spectrometer (Bruker Co., Germany) at

room temperature. Deuterochloroform was used as the solvent for P(BF-PBSS) and PBSS, and sulfuricacid-d_2 was used as the solvent for PBF.

Thermal transition temperature measurements were performed on a DSC-Q200 (TA Instruments, USA). The scans were recorded using a heating and cooling rate 10 °C min^{-1} from in a range of −75 °C to 200 °C under a N_2 atmosphere. Thermogravimetric analysis (TGA) was carried out on a TA Q50 (TA Instruments, USA) from 40 °C to 600 °C at a heating rate of 20 °C min^{-1} under a N_2 atmosphere. X-ray diffraction measurements were conducted on a D8 ADVANCE X-ray diffractometer (Bruker Co., Germany) in a 2θ range of 5–40° at a scan speed of 2.5° min^{-1}.

Dynamic mechanical analysis (DMA) was carried out using a DMA Q850 (TA Instruments, USA) from −100 °C to 130 °C at a heating rate of 3 °C min^{-1} with a tension mode of 1 Hz. The mechanical properties were evaluated with dumbbell-shaped samples according to ASTM D412 specifications using an INSTRON 3365 testing machine (Instron Co. Ltd, USA) with a crosshead speed of 20 mm min^{-1} at 25 °C. For each sample, at least five specimens were tested.

In vitro cytotoxicity testing using L929 mouse fibroblast cells was carried out by the Cell Counting Kit-8 (CCK-8) assay. The samples were sterilized and incubated in Dulbecco's modified Eagle's medium (DMEM) at a concentration of 0.5 g mL^{-1} for 72 h at 37 °C. The extract solution was filtered, and 10% fetal bovine serum was added. L929 cells were grown in DMEM at a density of 5.0×10^4 mL^{-1} and incubated in 5% CO_2 under humidified conditions at 37 °C. After 24 h, the medium was replaced by the prepared extract dilution, which was used as the new culture medium, and the initial medium was used as a negative control. The cells were allowed to proliferate for two or three days, and the number of viable cells was determined by adding 10 μL CCK-8 into the culture medium. After a further 1 h incubation, the absorbance at 450 nm was determined. All the sample extracts were tested at least three times to obtain average results. The relative growth rate (RGR) was calculated as follows:

$$\mathrm{RGR} = (A_{\mathrm{test}} - A_0)/(A_{\mathrm{control}} - A_0) \quad (2)$$

Here, A_{test} is the absorbance of the sample, A_{control} is the absorbance of the controlled well containing cells with DMEM, and A_0 is the absorbance of the solution containing only DMEM.

P(BF-PBSS) films of 2 × 2 cm in size and 0.5 mm thickness, were placed in vials containing phosphate buffer solution (pH = 7.4) at 37 °C. The media were replaced every 5 days. For every 10 d interval, the films were washed with distilled water, dried under vacuum at 40 °C and weighted until constant weight. The degree of biodegradation was estimated from the weight loss.

3. Results and discussion

A series of biobased P(BF-PBSS)s were synthesized *via* copolymerization of DMFD, BDO and PBSS. All the reacting monomers can be obtained from renewable biomass feedstocks. The designed P(BF-PBSS)s had both a stiff and a soft segment, and their properties could be tailored by changing the proportions of PBF and PBSS according to the desired application. The preparation of P(BF-PBSS)s and their structure are illustrated in Scheme 1. The obtained P(BF-PBSS)s exhibited number-average molecular weights from 17 000 to 31 000 and polydispersity index ranging from 1.32 to 1.72. The GPC curves and related data are shown in Fig. S1† and Table 1.

3.1. Microstructural characterization of P(BF-PBSS)s

The detailed chemical structures of P(BF-PBSS)s were characterized by ^{1}H-NMR, and ^{13}C-NMR. Because PBF is insoluble in common deuterated solvents, the ^{1}H- and ^{13}C-NMR spectra of PBF were recorded using dideuterosulfuric acid as the solvent, whereas those of P(BF-PBSS)s were recorded using deuterochloroform. Fig. 1 shows the ^{1}H-NMR spectra of PBF and P(BF-PBSS)s. For PBF, the signal at 6.93 ppm (c) is the characteristic absorption peak of C***H*** in the furan ring, and the signals at

Table 1 Molecular characteristics and composition of PBF and P(BF-PBSS)s

Samples	M_n[a]	M_w[a]	PDI[a]	Molar ratio PBF/PBSS[b]
PBF	22332	29542	1.32	—
P(BF-EF)-10	24227	38420	1.59	0.89/0.11
P(BF-EF)-20	22842	36442	1.60	0.78/0.12
P(BF-EF)-30	30895	53229	1.72	0.70/0.30
P(BF-EF)-40	19001	29549	1.56	0.59/0.41
P(BF-EF)-50	17141	25951	1.51	0.48/0.52

[a] Number- and weight-average molecular weights (M_n and M_w) and polydispersity index (PDI) determined by GPC. [b] Molar ratio determined by ^{1}H-NMR.

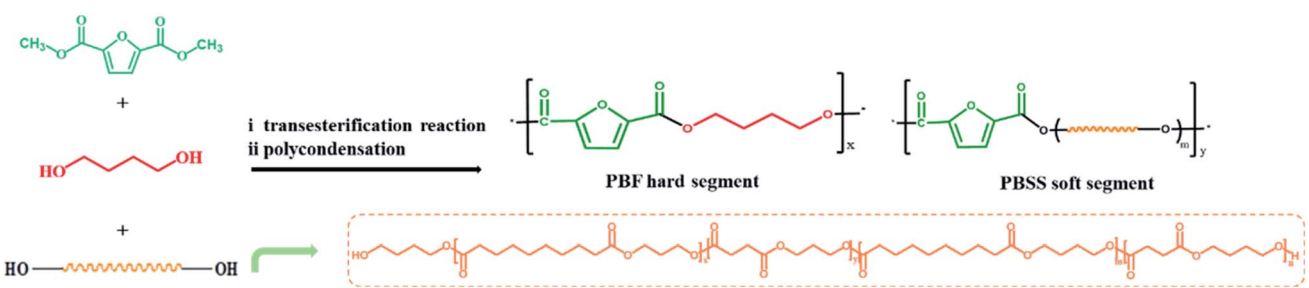

Scheme 1 Polymerization reactions leading to P(BF-PBSS)s.

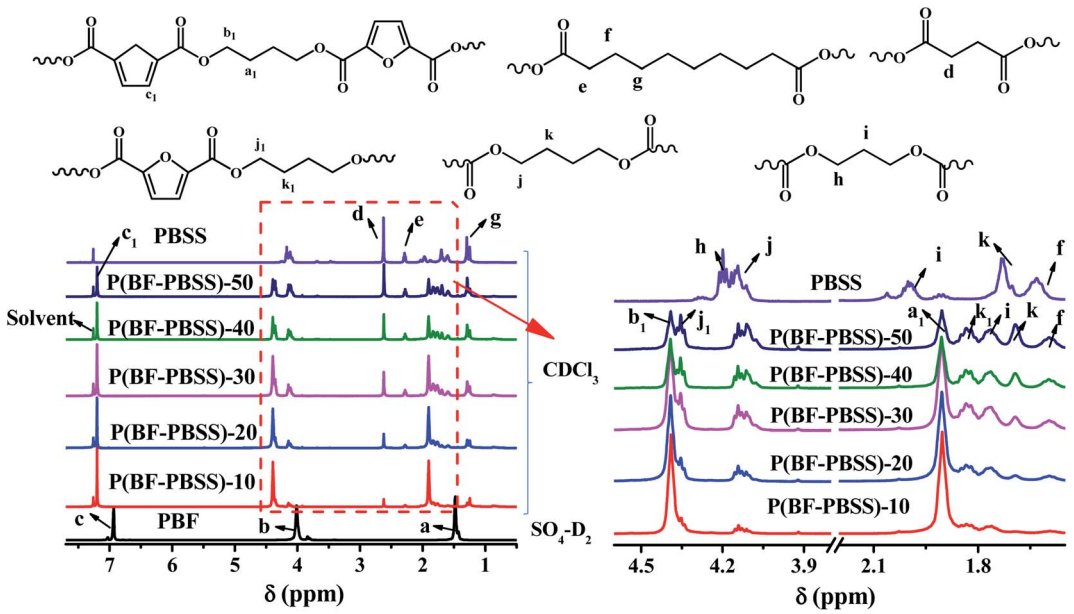

Fig. 1 ^{1}H-NMR spectra of PBF and P(BF-PBSS)s.

4.01 ppm (b) and 1.48 ppm (a) are the characteristic absorption peaks of O–C$\underline{H}_2$–(C$\underline{H}_2$)$_2$ in the butanediol structural units. For P(BF-PBSS)s, the main resonances associated with the PBF segment were those at 7.20 ppm (c_1), 4.39 ppm (b_1) and 1.91 pm (a_1), which can be attributed to the C$\underline{H}$ of the furan ring, and the O–C$\underline{H}_2$–(C$\underline{H}_2$)$_2$ in the butanediol structural unit. Compared with PBF, a number of chemical shifts corresponding to the characteristic PBSS proton peaks were presented in the P(BF-PBSS)s, as can be observed in Fig. 1b. The detailed absorption peaks derived from PBSS can be summarized as follows: the peak around 2.62 ppm (d) was attributed to the protons of the succinate structural unit (OOC–(C$\underline{H}_2$)$_2$); the peaks at 2.28 ppm (e), 1.61 ppm (f), and 1.29 ppm (g) were the protons of the sebacate structural unit (OOC–C$\underline{H}_2$–C$\underline{H}_2$–(C$\underline{H}_2$)$_4$); the peaks around 4.14 ppm (h) and 1.76 ppm (i) were the protons of the propanediol structural unit (O–C$\underline{H}_2$–C$\underline{H}_2$); and the peaks around 4.11 ppm (j) and 1.69 ppm (k) were the protons of the butanediol structural unit (O–C$\underline{H}_2$–C$\underline{H}_2$). Besides, some absorption peaks at around 4.35 ppm (j_1) and 1.83 ppm (k_1) was observed, which is the main resonance of butanediol structural unit neighboring the furan ring derived from PBSS. The presence of the above mentioned chemical shifts demonstrates the successful synthesis of P(BF-PBSS)s containing PBSS soft segments and PBF hard segments.

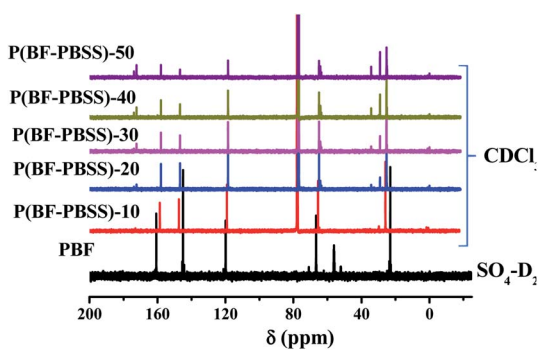

Fig. 2 ^{13}C-NMR spectra of PBF and P(BF-PBSS)s.

It can also be seen from Fig. 2 that the intensities of the characteristic absorption peaks for the PBSS segments (such as the chemical shifts at 4.14 ppm, 4.11 ppm, 2.62 ppm, 2.28 ppm, *etc.*) increased in relation to increasing PBSS content, whereas the intensities of the PBF absorption peaks (such as the chemical shifts at 7.20 ppm, 4.39 ppm, and 1.90 ppm) segments decrease in this respect. Additionally, the molar ratio of PBF to PBSS is given in Table 1. The real molar percentage of PBSS in the resulting P(BF-PBSS)s is increased with increasing of PBSS content. These results indicate that a higher PBSS content resulted in a higher content of PBSS soft segment in the P(BF-PBSS)s.

^{13}C-NMR analysis was also used to confirm the chemical structures of PBF and P(BF-PBSS)s. As shown in Fig. 2, the signals at 118 ppm, 145 ppm, and 160 ppm in PBF can be assigned to = $\underline{C}$H, $\underline{C}$–O, and $\underline{C}$OO, and in the furan ring. At the same time, the chemical shifts at 23 ppm and 66 ppm can be attributed to $\underline{C}$H$_2$–$\underline{C}$H$_2$–O of the butanediol structural unit. Compared with PBF, P(BF-PBSS)s exhibited many of the characteristic PBSS peaks. The chemical shift of $\underline{C}$OO in the PBSS segments appeared at 173 ppm, and the signals at 25 ppm, 29 ppm, 34 ppm, and 64–65 ppm could be assigned to $\underline{C}$H$_2$ in the PBSS segments. The ^{13}C-NMR results also demonstrate that a larger amount of PBSS soft segment was incorporated in P(BF-PBSS)s when the PBSS content was increased.

3.2. Thermal properties of P(BF-PBSS)s

Because of the possibility of decomposition of materials during processing and molding, the thermal stability of P(BF-PBSS)s is

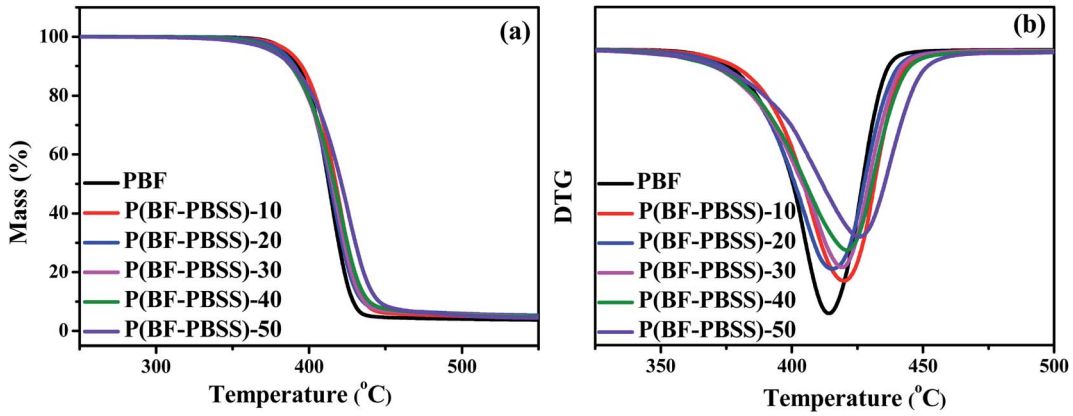

Fig. 3 TGA thermograms of PBF and P(BF-PBSS)s: (a) remaining mass and (b) first derivative of mass loss.

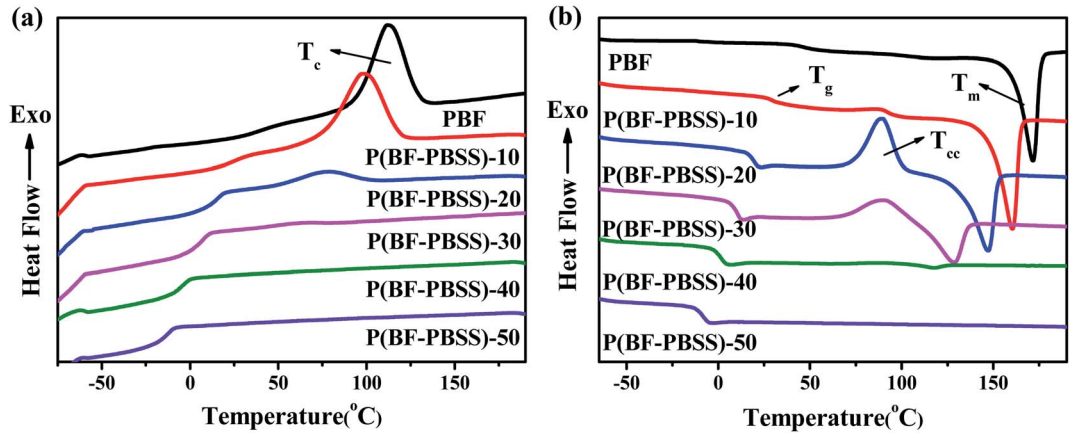

Fig. 4 DSC traces of PBF and P(BF-PBSS)s: (a) cooling curves and (b) second heating curves.

important and was investigated herein by the thermogravimetric analysis (TGA), where their TGA and DTG (differential TG) traces are presented in Fig. 3. The values for the onset decomposition temperature at 5% weight loss ($T_{d,5\%}$) and the maximum decomposition temperature ($T_{d,max}$) are summarized in Table S1.† In terms of TGA traces (Fig. 3), P(BF-PBSS)s and PBF degraded with only one stage of weight loss associated with the random chain scission mechanism of the ester bonds. Further, all the P(BF-PBSS)s exhibited a $T_{d,5\%}$ above 375 °C. P(BF-PBSS)s with a higher PBSS content presented a slightly lower $T_{d,5\%}$ compared with those with a lower PBSS content, which is consistent with the trend previously demonstrated by the PBF-PTMG system.[47] In addition, the $T_{d,max}$ values of P(BF-PBSS)s were around 420 °C, and there were no significant change in relation to PBSS content. The good thermal stability demonstrated that they can be processed safely at a relatively high temperature above their melting points, thus meeting the requirements of most applications.

The incorporation of PBSS soft segments for the formation of segmented block copolymers altered the thermal behaviors of P(BF-PBSS)s. The DSC traces of PBF and P(BF-PBSS)s are presented in Fig. 4. Related thermal transition data, including glass transition temperature (T_g), crystallization temperature (T_c), crystallization enthalpy (ΔH_c), melting temperature (T_m), melting enthalpy (ΔH_m), cold crystallization temperature (T_{cc}), and cold crystallization enthalpy (ΔH_{cc}), are shown in Table S1.† PBF demonstrated a T_c of 112 °C along its cooling curve, and a T_m of 171 °C along its heating curve. PBF is a semicrystalline copolyester with good crystallizability owing to its structural regularity and its chain flexibility. In Fig. 4, three kinds of thermal behavior can be observed in the P(BF-PBSS)s: (i) P(BF-PBSS)-10 and P(BF-PBSS)-20 crystallized at 98 °C and 77 °C along their cooling curves, and recrystallized at 87 °C and 89 °C and melted at 160 °C and 147 °C along their heating curves, respectively; (ii) P(BF-PBSS)-30 and P(BF-PBSS)-40 displayed no distinct crystallization peaks along its cooling curve, and exhibited T_{cc} at 90 °C and 87 °C and T_m at 128 °C and 117 °C along its heating curve, respectively; and (iii) P(BF-PBSS)-50 displayed neither crystallization nor melting peaks along either their cooling or heating curves. Apparently, the incorporation of an additional PBSS soft segment disturbed the regularity of the PBF polymer chains, and the crystallization ability of the P(BF-PBSS)s was significantly depressed. A higher PBSS content shortened the lengths of the PBF segments, inducing more defects in the PBF crystals, decreasing the thickness of the lamella, and lowering the corresponding T_c, ΔH_c, T_m, and ΔH_m

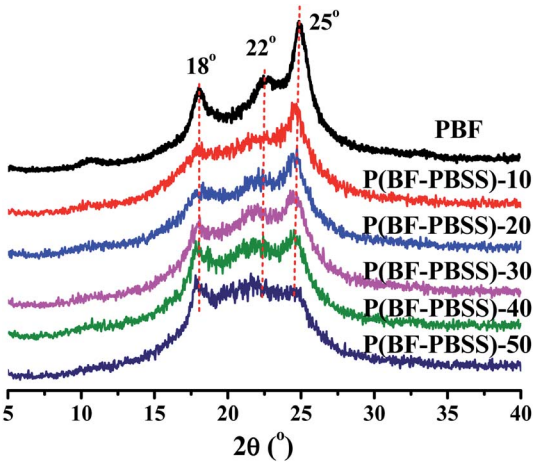

Fig. 5 WXRD curves of PBF and P(BF-PBSS)s.

values. When the amount of PBSS was higher than 40 wt%, the P(BF-PBSS)s does not crystallize at all according to the DSC and is completely amorphous. Similar results have also been observed in other TPEE systems.[35,37]

The P(BF-PBSS)s each had a single T_g, which decreased from 48 °C to −6 °C with increasing PBSS content. The presence of the PBSS soft segments promoted chain mobility in the P(BF-PBSS)s, contributing to a lower T_g compared with that of PBF. These results indicate that the PBF and PBSS segments are to some extent compatible. These results also demonstrate that the melting/crystallization behavior of P(BF-PBSS)s is associated with the stiff PBF segment, whereas the glass transition of P(BF-PBSS)s is related to their soft PBSS segments. Consequently, the thermal behavior of the P(BF-PBSS)s can thus be tuned by controlling the ratio of PBF to PBSS.

3.3. Crystal structure

Wide-angle X-ray diffraction was used to further evaluate the crystallization behavior of P(BF-PBSS)s. As shown in Fig. 5, P(BF-PBSS)s exhibited strong diffraction peaks at 18°, 22°, and 25°, which is consistent with the characteristic PBF diffraction peaks.[36] No diffraction peaks other those of PBF were found in the P(BF-PBSS)s, indicating that the introduction of the PBSS segment did not change the crystal structure of PBF. However, the intensities of the diffraction peaks were gradually weakened as the content of PBSS increased, which is in close agreement with previous DSC results. By deconvolution of the diffraction patterns, the crystallinity of P(BF-PBSS)s can be calculated. As shown in Table S1,† the crystallinity of P(BF-PBSS)s decreased from 29.4% to 12.6% with increasing PBSS content, because incorporation of the PBSS soft segment disturbed the regularity of the PBF polymer chains.

3.4. Dynamic mechanical properties

Generally, the microphase separation in TPEEs, is induced by crystallization of their hard segments. TPEEs actually contain four phases, a crystalline hard segment, an amorphous hard segment, an amorphous soft segment, and one that is a mixture of the amorphous hard and soft segments. For traditional TPEEs such as PBT-PTMG, three thermal transitions can be observed. The first is the melting temperature of the crystalline hard segment, and the other two are the glass transitions of the amorphous hard segment and the amorphous soft segment, respectively. The two glass transition temperatures usually shift and merge to form a broad peak in relation to increasing thermodynamic miscibility of the two amorphous domains.[35]

The dynamic mechanical properties of PBF and P(BF-PBSS)s were investigated by DMA, and the dependences of loss factor (tan δ) and storage modulus (E') on temperature are shown in Fig. 6. In Fig. 6a, a broad peak belonged to glass transition was observed for P(BF-PBSS)s, indicating that the P(BF-PBSS)s contained a single amorphous phase consisting of both amorphous PBSS and amorphous PBF. The peak of tan δ decreased along the PBSS content, owing to the progressive increase in chain flexibility. These results are in line with the T_g values determined by DSC, although there were some deviations in the DSC and DMA tests of the same samples. Under different determination conditions, the motility of polymer chain segments is different, so the T_g of the polymers obtained by various methods is different.

In addition, the shoulder appeared on the high-temperature side for PBF and P(BF-PBSS)-10, which may be attributed to the

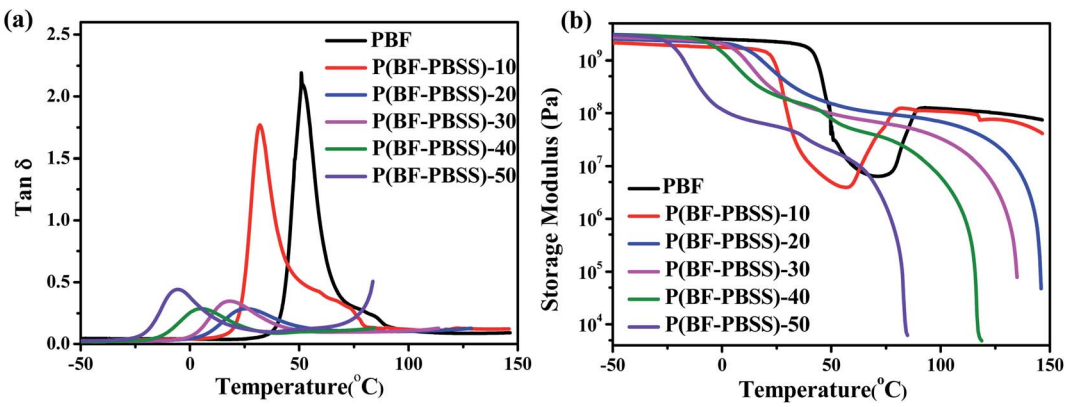

Fig. 6 DMA curves of PBF and P(BF-PBSS)s: (a) tan δ and (b) storage modulus.

cold crystallization during heating process. Corresponding, the E' increased at 73–90 °C for PBF and at 55–78 °C for P(BF-PBSS)-10. It can thus be concluded that the P(BF-PBSS)s possessed two phases rather than four. One phase was the crystalline domain of the PBF hard segments, and the other was the mixture of amorphous PBSS and amorphous PBF. As a result, the microphase separation of P(BF-PBSS)s was mainly induced by crystallization of the hard segments.

3.5. Mechanical properties

Tensile tests were performed to investigate the mechanical properties of P(BF-PBSS)s. The stress–strain curves of PBF and P(BF-PBSS)s are depicted in Fig. 7. As expected, incorporation of PBSS into the copolyesters significantly changed their mechanical properties. In particular, their tensile strength decreased, whereas the elongation at break first increased and then decreased with increasing PBSS content. As shown in Fig. 7, PBF and P(BF-PBSS)-10 were a typical hard and ductile semicrystalline plastics with distinctive points and strain-hardening behavior. When PBSS was incorporated, their tensile strength was reduced from 49 to 30 MPa, whereas the elongation at break was slightly decreased. As the PBSS content increased from 20 wt% to 30 wt%, P(BF-PBSS)-20 and P(BF-PBSS)-30 behaved like thermoplastic elastomers, demonstrating no yielding/necking but broad rubber plateaus and stress hardening. When the PBSS content was further increased from 40 wt% to 50 wt%, the tensile strength and elongation at break of the P(BF-PBSS)s decreased significantly. The above results can be in large part attributed to chain rigidity. The addition of the PBSS segment caused a loss of regularity along the chain, and the consequent decrease in the crystallinity of P(BF-PBSS)s is expected resulted in decreases in modulus and strength. In particular, P(BF-PBSS)-20 exhibited a high elongation at break (~1100%) and a relatively high tensile strength (34 MPa). The coexistence of the rigid furan ring and the flexible PBSS unit in the chain structure and the amorphous feature may have contributed to the unique mechanical properties of P(BF-PBSS)-20. Compared with some other biobased TPEE systems, P(BF-PBSS)s exhibit similar mechanical properties.[35,37,38] Altogether, it was found that the P(BF-PBSS)s could be modulated from crystalline thermoplastics with low PBSS content to elastomer-like polymers with high PBSS content.

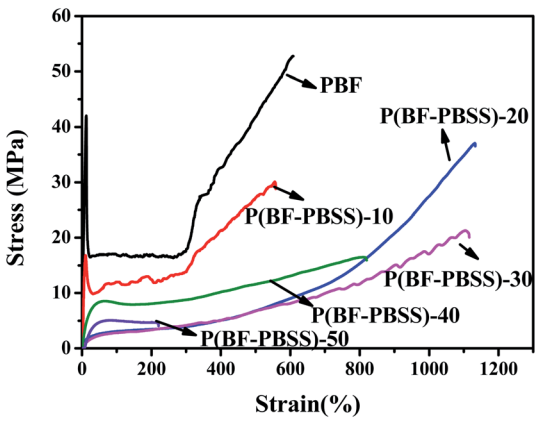

Fig. 7 Strain–stress curves of PBF and P(BF-PBSS)s.

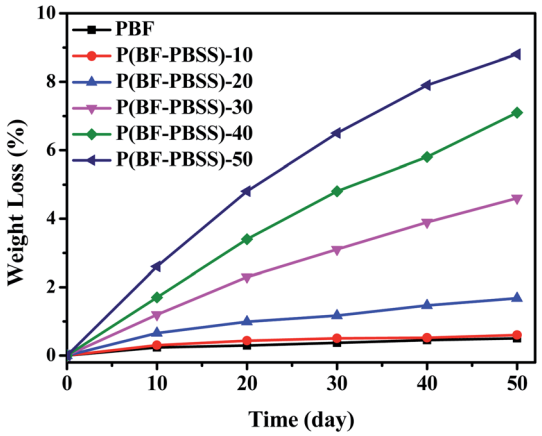

Fig. 8 Weight loss of PBF and P(BF-PBSS)s soaking in PBS solution.

3.6. Cytocompatibility and degradability

Determining the cytotoxicity of a material is the first step in establishing whether it is suitable for biomedical applications. Cytotoxicity tests of the P(EF-PBSS)s were undertaken *via* the L929 cells in the extract. The cell RGR values calculated from the optical density values are displayed in Fig. S2.† The cytotoxicities of the materials can be classified into six grades based on the RGR values, as shown in Table S2.† A material with grades 0 or 1 has very low or no cytotoxicity to L929 cells and is thus qualified for use in biomedicine. A material with grade 2 has low cytotoxicity, but should be further examined by considering cell morphology. All the other grades indicate that the material is unqualified for biomedical use because of its very high cytotoxicity. The RGR values of P(BF-PBSS)s were all higher than 95%, indicating low or no cytotoxicity to L929 cells. These results demonstrate that our biobased P(BF-PBSS)s have acceptable biocompatibility and could potentially be used as biomedical materials.

The degradability of P(BF-PBSS)s was tested in PBS solution, and weight loss of P(BF-PBSS)s is shown in Fig. 8. PBF and P(BF-PBSS)-10 displayed nearly no weight loss. The weight loss of P(BF-PBSS) slightly increased with increasing of soaking time and PBSS content. P(BF-PBSS)-50 shows a weight loss of 8.9% after 50 days. Although the introduction of PBSS units accelerated the degradability, the hydrolysis rate of P(BF-PBSS) was relatively slower.

4. Conclusion

Biobased TPEEs (P(BF-PBSS)s) were successfully synthesized by the polymerization by dimethyl-2,5-furandicarboxylate, 1,4-butanediol, and synthetic low-molecular-weight biobased polyester. The as-prepared P(BF-PBSS)s contained the PBF as their hard segment and PBSS as their soft segment, and their performance could be tailored by tuning the proportion of PBF and PBSS for the desired application. The number-average molecular weight and polydispersity of the P(BF-PBSS)s

ranged from 17 000 to 31 000 and from 1.32 to 1.72, respectively. The microstructures of the P(BF-PBSS)s were confirmed by NMR. P(BF-PBSS)s demonstrated good thermal stability and had an onset decomposition temperature above 370 °C. Apparently, the incorporation of the PBSS soft segment shortened the length of the PBF segments and disturbed the regularity of the PBF polymer chains, resulting in a decrease in the crystallinity of the P(BF-PBSS)s. Interestingly, DMA indicated that the P(BF-PBSS)s comprised two domains: crystalline PBF and a mixture of amorphous PBF and PBSS. As a result, the microphase separation of P(BF-PBSS)s was mainly induced by the crystallization of PBF. More importantly, the P(BF-PBSS)s could be modulated from crystalline thermoplastics with low PBSS content to elastomer-like polymers with high PBSS content. In addition, P(BF-PBSS)-20 exhibited a high elongation at break (∼1100%) and a relatively high tensile strength (34 MPa). Moreover, the P(BF-PBSS)s demonstrated low or no cytotoxicity to L929 cells, and low degradation rate. The combination of sustainability, good mechanical properties, and noncytotoxicity makes these P(BF-PBSS)s potential candidates for high-strength biomedical materials.

Conflicts of interest

There are no conflicts to declare.

Acknowledgements

This work was supported by National Natural Science Foundation of China (No. 51703133), Program for Liaoning Innovative Talents in Universities of China (No. LR2019053), and Natural Science Foundation of Liaoning, China (No. 2019-MS-263).

References

1 R. Mülhaupt, Green polymer chemistry and bio-based plastics: dreams and reality, *Macromol. Chem. Phys.*, 2013, **214**(2), 159–174.
2 T. Iwata, Biodegradable and bio-based polymers: future prospects of eco-friendly plastics, *Angew. Chem., Int. Ed.*, 2015, **54**(11), 3210–3215.
3 A. Gandini, Polymers from renewable resources: a challenge for the future of macromolecular materials, *Macromolecules*, 2008, **41**(24), 9491–9504.
4 Y. Zhu, C. Romain and C. K. Williams, Sustainable polymers from renewable resources, *Nature*, 2016, **540**(7633), 354–362.
5 X. Pang, X. Zhuang, Z. Tang and X. Chen, Polylactic acid (PLA): research, development and industrialization, *Biotechnol. J.*, 2010, **5**(11), 1125–1136.
6 D. B. Hazer, E. Kılıçay and B. Hazer, Poly (3-hydroxyalkanoate) s: diversification and biomedical applications: a state of the art review, *Mater. Sci. Eng., C*, 2012, **32**(4), 637–647.
7 J. Xu and B. H. Guo, Poly (butylene succinate) and its copolymers: research, development and industrialization, *Biotechnol. J.*, 2010, **5**(11), 1149–1163.
8 R. J. Spontak and N. P. Patel, Thermoplastic elastomers: fundamentals and applications, *Curr. Opin. Colloid Interface Sci.*, 2000, **5**(5), 333–340.
9 R. J. Cella, Morphology of segmented polyester thermoplastic elastomers, *J. Polym. Sci., Polym. Symp.*, 1973, **42**(2), 727–740.
10 W. Gabriëlse, M. Soliman and K. Dijkstra, Microstructure and phase behavior of block copoly (ether ester) thermoplastic elastomers, *Macromolecules*, 2001, **34**(6), 1685–1693.
11 G. Holden, Thermoplastic elastomers, in *Rubber technology*, Springer, 1987, pp. 465–481.
12 W. Wang, W. Lu, A. Goodwin, H. Wang, P. Yin, N.-G. Kang, K. Hong and J. W. Mays, Recent advances in thermoplastic elastomers from living polymerizations: Macromolecular architectures and supramolecular chemistry, *Prog. Polym. Sci.*, 2019, **95**, 1–31.
13 Z. Wang, L. Yuan and C. Tang, Sustainable elastomers from renewable biomass, *Acc. Chem. Res.*, 2017, **50**(7), 1762–1773.
14 W. K. Witsiepe, Segmented thermoplastic copolyester elastomers, *US pat.*, 3651014A, 1972.
15 C. Zhou, Z. Wei, X. Lei and Y. Li, Fully biobased thermoplastic elastomers: synthesis and characterization of poly(l-lactide)-b-polymyrcene-b-poly(l-lactide) triblock copolymers, *RSC Adv.*, 2016, **6**(68), 63508–63514.
16 M. T. Martello and M. A. Hillmyer, Polylactide–poly (6-methyl-ε-caprolactone)–polylactide thermoplastic elastomers, *Macromolecules*, 2011, **44**(21), 8537–8545.
17 S. Lee, J. S. Yuk, H. Park, Y.-W. Kim and J. Shin, Multiblock thermoplastic elastomers derived from biodiesel, poly (propylene glycol), and l-Lactide, *ACS Sustainable Chem. Eng.*, 2017, **5**(9), 8148–8160.
18 D. K. Schneiderman, E. M. Hill, M. T. Martello and M. A. Hillmyer, Poly(lactide)-block-poly(ε-caprolactone-co-ε-decalactone)-block-poly(lactide) copolymer elastomers, *Polym. Chem.*, 2015, **6**(19), 3641–3651.
19 C. L. Wanamaker, M. J. Bluemle, L. M. Pitet, L. E. O'Leary, W. B. Tolman and M. A. Hillmyer, Consequences of Polylactide Stereochemistry on the Properties of Polylactide-Polymenthide-Polylactide Thermoplastic Elastomers, *Biomacromolecules*, 2009, **10**(10), 2904–2911.
20 C. L. Wanamaker, L. E. O'Leary, N. A. Lynd, M. A. Hillmyer and W. B. Tolman, Renewable-resource thermoplastic elastomers based on polylactide and polymenthide, *Biomacromolecules*, 2007, **8**(11), 3634–3640.
21 A. Watts, N. Kurokawa and M. A. Hillmyer, Strong, resilient, and sustainable aliphatic polyester thermoplastic elastomers, *Biomacromolecules*, 2017, **18**(6), 1845–1854.
22 M. T. Martello, D. K. Schneiderman and M. A. Hillmyer, Synthesis and melt processing of sustainable poly (ε-decalactone)-block-poly (lactide) multiblock thermoplastic elastomers, *ACS Sustainable Chem. Eng.*, 2014, **2**(11), 2519–2526.
23 T. Kobayashi and S. Matsumura, Enzymatic synthesis and properties of novel biodegradable and biobased thermoplastic elastomers, *Polym. Degrad. Stab.*, 2011, **96**(12), 2071–2079.

24 T. Yagihara and S. Matsumura, Enzymatic Synthesis and Chemical Recycling of Novel Polyester-Type Thermoplastic Elastomers, *Polymers*, 2012, **4**(2), 1259–1277.

25 Y. Liu, K. Yao, X. Chen, J. Wang, Z. Wang, H. J. Ploehn, C. Wang, F. Chu and C. Tang, Sustainable thermoplastic elastomers derived from renewable cellulose, rosin and fatty acids, *Polym. Chem.*, 2014, **5**(9), 3170–3181.

26 F. Fenouillot, A. Rousseau, G. Colomines, R. Saint-Loup and J.-P. Pascault, Polymers from renewable 1, 4: 3, 6-dianhydrohexitols (isosorbide, isomannide and isoidide): A review, *Prog. Polym. Sci.*, 2010, **35**(5), 578–622.

27 H. Zhou, H. Xu, X. Wang and Y. Liu, Convergent production of 2, 5-furandicarboxylic acid from biomass and CO 2, *Green Chem.*, 2019, **21**(11), 2923–2927.

28 H. Kang, M. Li, Z. Tang, J. Xue, X. Hu, L. Zhang and B. Guo, Synthesis and characterization of biobased isosorbide-containing copolyesters as shape memory polymers for biomedical applications, *J. Mater. Chem. B*, 2014, **2**(45), 7877–7886.

29 Z. Wei, C. Zhou, Y. Yu and Y. Li, Biobased copolyesters from renewable resources: synthesis and crystallization behavior of poly (decamethylene sebacate-co-isosorbide sebacate), *RSC Adv.*, 2015, **5**(53), 42777–42788.

30 A. F. Sousa, M. Matos, C. S. Freire, A. J. Silvestre and J. F. Coelho, New copolyesters derived from terephthalic and 2, 5-furandicarboxylic acids: A step forward in the development of biobased polyesters, *Polymer*, 2013, **54**(2), 513–519.

31 A. F. Sousa, C. Vilela, A. C. Fonseca, M. Matos, C. S. Freire, G.-J. M. Gruter, J. F. Coelho and A. J. Silvestre, Biobased polyesters and other polymers from 2, 5-furandicarboxylic acid: a tribute to furan excellency, *Polym. Chem.*, 2015, **6**(33), 5961–5983.

32 G. Z. Papageorgiou, D. G. Papageorgiou, Z. Terzopoulou and D. N. Bikiaris, Production of bio-based 2, 5-furan dicarboxylate polyesters: Recent progress and critical aspects in their synthesis and thermal properties, *Eur. Polym. J.*, 2016, **83**, 202–229.

33 S. Hong, K.-D. Min, B.-U. Nam and O. O. Park, High molecular weight bio furan-based co-polyesters for food packaging applications: synthesis, characterization and solid-state polymerization, *Green Chem.*, 2016, **18**(19), 5142–5150.

34 M. Kwiatkowska, I. Kowalczyk, K. Kwiatkowski, A. Szymczyk and Z. Rosłaniec, Fully biobased multiblock copolymers of furan-aromatic polyester and dimerized fatty acid: Synthesis and characterization, *Polymer*, 2016, **99**, 503–512.

35 D. Chi, F. Liu, H. Na, J. Chen, C. Hao and J. Zhu, Poly (neopentyl glycol 2, 5-furandicarboxylate): a promising hard segment for the development of bio-based thermoplastic poly (ether-ester) elastomer with high performance, *ACS Sustainable Chem. Eng.*, 2018, **6**(8), 9893–9902.

36 A. Sousa, N. Guigo, M. Pożycka, M. Delgado, J. Soares, P. Mendonça, J. Coelho, N. Sbirrazzuoli and A. Silvestre, Tailored design of renewable copolymers based on poly (1, 4-butylene 2, 5-furandicarboxylate) and poly (ethylene glycol) with refined thermal properties, *Polym. Chem.*, 2018, **9**(6), 722–731.

37 H. Xie, L. Wu, B.-G. Li and P. Dubois, Poly (ethylene 2, 5-furandicarboxylate-mb-poly (tetramethylene glycol)) multiblock copolymers: From high tough thermoplastics to elastomers, *Polymer*, 2018, **155**, 89–98.

38 M. Zheng, X. Zang, G. Wang, P. Wang, B. Lu and J. Ji, Poly (butylene 2, 5-furandicarboxylate-ε-caprolactone): A new bio-based elastomer with high strength and biodegradability, *eXPRESS Polym. Lett.*, 2017, **11**(8), 611–621.

39 J. C. Morales-Huerta, C. B. Ciulik, A. M. de Ilarduya and S. Muñoz-Guerra, Fully bio-based aromatic–aliphatic copolyesters: poly(butylene furandicarboxylate-co-succinate)s obtained by ring opening polymerization, *Polym. Chem.*, 2017, **8**(4), 748–760.

40 Q. Ouyang, J. Liu, C. Li, L. Zheng, Y. Xiao, S. Wu and B. Zhang, A facile method to synthesize bio-based and biodegradable copolymers from furandicarboxylic acid and isosorbide with high molecular weights and excellent thermal and mechanical properties, *Polym. Chem.*, 2019, **10**(41), 5594–5601.

41 Z. Terzopoulou, E. Karakatsianopoulou, N. Kasmi, V. Tsanaktsis, N. Nikolaidis, M. Kostoglou, G. Z. Papageorgiou, D. A. Lambropoulou and D. N. Bikiaris, Effect of catalyst type on molecular weight increase and coloration of poly(ethylene furanoate) biobased polyester during melt polycondensation, *Polym. Chem.*, 2017, **8**(44), 6895–6908.

42 H. Hu, R. Zhang, J. Wang, W. B. Ying, L. Shi, C. Yao, Z. Kong, K. Wang and J. Zhu, A mild method to prepare high molecular weight poly(butylene furandicarboxylate-co-glycolate) copolyesters: effects of the glycolate content on thermal, mechanical, and barrier properties and biodegradability, *Green Chem.*, 2019, **21**(11), 3013–3022.

43 T. Wei, L. Lei, H. Kang, B. Qiao, Z. Wang, L. Zhang, P. Coates, K. C. Hua and J. Kulig, Tough Bio-Based Elastomer Nanocomposites with High Performance for Engineering Applications, *Adv. Eng. Mater.*, 2012, **14**(1-2), 112–118.

44 H. Kang, X. Li, J. Xue, L. Zhang, L. Liu, R. Xu and B. Guo, Preparation and characterization of high strength and noncytotoxic bioelastomers containing isosorbide, *RSC Adv.*, 2014, **4**(37), 19462–19471.

45 X. Hu, H. Kang, Y. Li, M. Li, R. Wang, R. Xu, H. Qiao and L. Zhang, Direct copolycondensation of biobased elastomers based on lactic acid with tunable and versatile properties, *Polym. Chem.*, 2015, **6**(47), 8112–8123.

46 Q. Liu, L. Jiang, R. Shi and L. Zhang, Synthesis, preparation, in vitro degradation, and application of novel degradable bioelastomers—A review, *Prog. Polym. Sci.*, 2012, **37**(5), 715–765.

47 W. Zhou, Y. Zhang, Y. Xu, P. Wang, L. Gao, W. Zhang and J. Ji, Synthesis and characterization of bio-based poly (butylene furandicarboxylate)-b-poly (tetramethylene glycol) copolymers, *Polym. Degrad. Stab.*, 2014, **109**, 21–26.